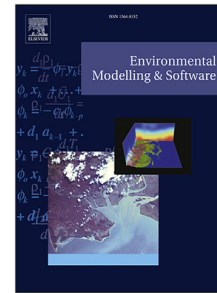


Journal Pre-proof

Automated marine litter investigation for underwater images using a zero-shot pipeline

Tri-Hai Nguyen, Minh Dang



PII: S1364-8152(24)00126-9

DOI: <https://doi.org/10.1016/j.envsoft.2024.106065>

Reference: ENSO 106065

To appear in: *Environmental Modelling and Software*

Received date: 22 January 2024

Revised date: 28 April 2024

Accepted date: 5 May 2024

Please cite this article as: T.-H. Nguyen and M. Dang, Automated marine litter investigation for underwater images using a zero-shot pipeline. *Environmental Modelling and Software* (2024), doi: <https://doi.org/10.1016/j.envsoft.2024.106065>.

This is a PDF file of an article that has undergone enhancements after acceptance, such as the addition of a cover page and metadata, and formatting for readability, but it is not yet the definitive version of record. This version will undergo additional copyediting, typesetting and review before it is published in its final form, but we are providing this version to give early visibility of the article. Please note that, during the production process, errors may be discovered which could affect the content, and all legal disclaimers that apply to the journal pertain.

© 2024 Elsevier Ltd. All rights reserved.

Automated Marine Litter Investigation for Underwater Images using a Zero-shot Pipeline

Tri-Hai Nguyen^a, Minh Dang^{b,c,*}

^aFaculty of Computer Science, Ho Chi Minh City Open University, Ho Chi Minh City 700000, Vietnam

^bInstitute of Research and Development, Duy Tan University, Da Nang 550000, Vietnam

^cFaculty of Information Technology, Duy Tan University, Da Nang 550000, Vietnam

Abstract

Accurate and automated identification of marine litter on the seafloor is crucial due to its detrimental effects on marine ecosystems. While advancements in underwater imaging have facilitated this task, the significant human involvement required in traditional approaches necessitates the development of more efficient and cost-effective solutions. This study presents an efficient zero-shot segmentation framework based on Segment-Anything (SAM) guided by Interpretable Contrastive Language-Image Pre-training (iCLIP) for identifying and segmenting eight common seafloor litter categories in realistic underwater environments without model training. The framework supports prompt input by design, which allows it to transfer its zero-shot capabilities to new types of marine litter. To further improve the framework's performance, two additional components were incorporated: an underwater image enhancement model that addresses the degraded image quality common in underwater environments, and a mask post-processing algorithm that reduces noise masks generated by the framework. The recorded mean intersection over union (mIOU) of 69.9% on the testing dataset suggested that zero-shot approaches have the potential to become a valuable technique for automatically detecting marine litter during surveys and enabling continuous and accurate litter monitoring.

Keywords: deep learning, zero-shot, marine litter, segmentation, waste management

*Corresponding author

Email address: danglienminh@duytan.edu.vn (L. Minh Dang)

1. Introduction

Marine debris, also known as marine litter or ocean trash, is a wide range of human-made waste that enters oceans, seas, and other water bodies. It includes items such as plastics, glass, metals, paper, textiles, and other materials, both macroscopic and microscopic. Marine debris is a pressing global environmental problem with far-reaching consequences for marine life, habitats, ecosystems, economies, and human health (Iñiguez et al., 2016). It harms marine creatures that can ingest or become entangled in debris, leading to injuries, suffocation, or death. The entanglement and ingestion of debris can disrupt the reproductive cycles and feeding habits of marine creatures, potentially impacting the abundance and quality of seafood available for human consumption (Jang et al., 2020). Additionally, it affects human health due to the consumption of seafood contaminated by litter. The sources and accumulation patterns of marine litter are highly diverse, influenced by factors such as geographical location, industrial activities, waste management practices, and human behavior. These multifaceted factors contribute to the complexity of the issue, necessitating comprehensive solutions (Jia et al., 2023; Galgani et al., 2019).

The growing technological capabilities of underwater observation technologies and computer vision advancements have led to the widespread adoption of photography-based monitoring for assessing the type, distribution, and abundance of marine litter (Radeta et al., 2022). This approach provides valuable insights into the severity of marine litter pollution, enabling the development of effective cleanup programs and fostering public awareness campaigns to reduce litter generation (Politikos et al., 2021; Kraft et al., 2021). The detection of seafloor litter in real-world underwater video footage presents a complex challenge due to the diverse and dynamic nature of marine environments (Jian et al., 2021). Video footage can exhibit varying lighting conditions, zoom levels, and camera angles, often causing marine litter to be barely visible (Raveendran et al., 2021). Moreover, the sheer variety of litter types, the diverse shapes within the same type of litter, the degradation of litter over time, its potential burial in the seabed, and the presence of complex background like rocks and seagrass can easily mislead detection algorithms (Schneider et al., 2018; Mæland and Staupe-Delgado, 2020). The development of algorithms capable of automatically detecting marine litter in underwater images would support analytical processes and play an imperative role in improving understanding of marine

29 pollution and motivating targeted mitigation and management strategies (Sandra et al., 2023).

30 Deep learning (DL) has emerged as a powerful tool for image understanding across various domains,
31 including computer vision (Marin et al., 2021), natural language processing, recommender system, and
32 anomaly detection. Object segmentation, a subfield of DL, extends beyond object recognition by
33 localizing, classifying, and segmenting objects within images (Minh et al., 2022). In recent efforts,
34 researchers have implemented existing object segmentation models to identify the position of marine
35 litter (Zhou et al., 2022; Teng et al., 2022; Chin et al., 2022), while others have focused on strengthening
36 backbone networks to enhance marine litter feature extraction (Politikos et al., 2021; Corrigan et al.,
37 2023). Additionally, several studies have suggested efficient and lightweight DL structures fine-tuned
38 for marine litter detection (Deng et al., 2021; Ma et al., 2023). Despite these advancements, the
39 supervised marine litter recognition approach still faces limitations. Models trained on a finite set of
40 classes often exhibit restricted performance when encountering novel classes (Madricardo et al., 2020).
41 This limitation stems from the reliance on labeled data, which can be scarce and expensive to acquire
42 for the vast diversity of marine litter categories.

43 Zero-shot learning is a transformative machine learning (ML) paradigm that enables models to rec-
44 ognize classes or categories they have never encountered during the training phase (Sun et al., 2021).
45 By leveraging a broader set of related information during training, ZSL enables models to generalize
46 and make predictions for unseen or novel classes. The Segment Anything Model (SAM) (Kirillov et al.,
47 2023), developed by Meta AI, represents a pioneering method in image segmentation, demonstrating
48 remarkable generalization capabilities across various benchmark datasets without the need for addi-
49 tional training on unseen objects. ZSL holds particular promise for marine litter recognition due to
50 the vast diversity of marine litter types and the challenges associated with collecting labeled data
51 for each (Raveendran et al., 2021; Schneider et al., 2018). The development of an automatic marine
52 litter recognition framework powered by ZSL has the potential to revolutionize litter assessment by
53 providing a faster, more cost-effective alternative to standard manual data analysis approaches.

54 Therefore, the need for an efficient and accurate system for segmenting underwater objects is es-
55 sential for the identification and cleanup of marine litter. This paper proposes a zero-shot pipeline for
56 deep learning-based marine litter segmentation that overcomes the challenges of limited labeled data

57 and complex seafloor environments. Our contributions include: (1) using underwater image enhance-
58 ment (UIE) algorithms to improve dataset image quality; (2) developing a zero-shot segmentation
59 approach based on SAM guided by Interpretable Contrastive Language–Image Pre-training (iCLIP)
60 algorithms, which eliminates the need for manual data annotation; and (3) demonstrating that the pro-
61 posed framework achieves comparable segmentation performance and inference speed to the supervised
62 approach.

63 The remainder of this paper is organized as follows. Section 2 introduces the large-scale marine
64 litter dataset. Section 3 presents the zero-shot marine litter segmentation pipeline in detail. Section
65 4 evaluates the proposed approach on experimental data and discusses the obtained results of the
66 zero-shot segmentation approach. Finally, Section 5 concludes the paper with some remarks.

67 2. Marine litter dataset

68 Previous marine litter studies have been limited by small datasets with few litter types. For
69 example, the seafloor marine litter dataset (635 images) (Politikos et al., 2021), the JAMSTEC dataset
70 (5352 images) (dat), and the DSDebris dataset (15K images) (Huang et al., 2023). As a result, this
71 study uses a massive dataset of around 112K images that cover eight common marine litter types,
72 surpassing previous datasets in both quantity and quality. Although the specific composition of marine
73 litter can vary depending on geographical location and dominant industries, the chosen categories in
74 the dataset represent a significant portion of debris found globally (Politikos et al., 2021; Huang et al.,
75 2023), making it relevant for various coastal monitoring and cleanup scenarios.

76 The dataset was shared by the National Information Society Agency of Korea (NIA) for research
77 purposes¹. It was mainly collected by Pukyong Ocean Technology Co., Ltd. and labeled by the
78 Pukyong University Industry-Academia Cooperation Division². The marine litter dataset was collected
79 using a commercial GoPro5 action camera (gop). Eight surveys were conducted to assess seafloor litter,
80 covering more than 100 hectares of seafloor over 8 hours of underwater video footage. The collection
81 was planned for cloudless days between 11:00 AM and 1:00 PM, during solar noon, to ensure the best

¹<https://aihub.or.kr/>

²<https://www.pknu.ac.kr/eng>

82 contrast and clarity in the videos. Video frames with high turbidity, color shifts, or light flares were
 83 excluded from the analysis. Each image is 1920×1080 pixels at 96 dpi. Sample images for each litter
 84 type are shown in Figure 1. A total of 111,890 images were collected and annotated, of which 89,512
 85 (80%) were used for training and validation, and 22,378 (20%) for testing.

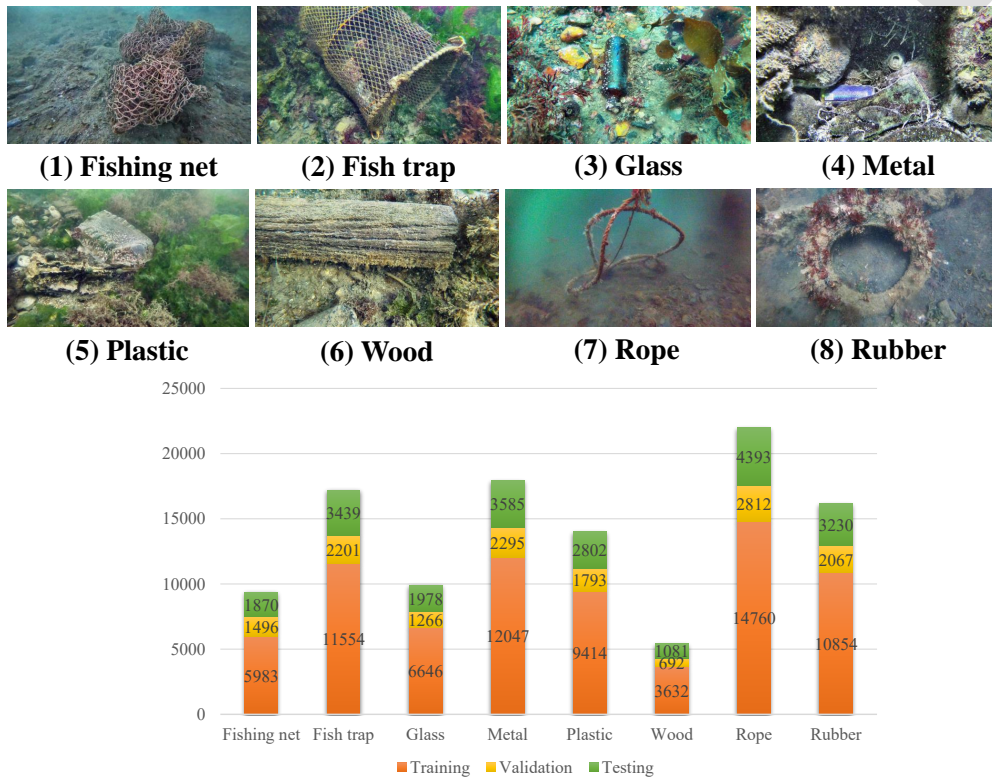


Figure 1: Visual representation of the eight most common types of marine litter in the dataset and a bar chart depicting the distribution of training, validation, and testing images across different marine litter types.

86 3. Methodology

87 3.1. Image pre-processing

88 Previous studies have shown that aquatic datasets often suffer from challenges such as poor lighting,
 89 color distortion, low contrast, and reduced visibility due to light scattering and absorption in water.
 90 These challenges can significantly degrade the performance of litter identification models during train-

91 ing (Radeta et al., 2022). Underwater image enhancement (UIE) is a common technique that can
92 be implemented to mitigating these issues. UIE is essential for improving the performance of image
93 recognition models, as it reduces the gap between the underwater and the terrestrial domains and
94 enhances the discriminative features of the objects (Huang and Belongie, 2017).

95 UIE aims to improve the visual quality of images captured in underwater environments, where fac-
96 tors like light attenuation, scattering, and color distortion severely degrade image clarity (Raveendran
97 et al., 2021). One common approach involves the restoration of images using various noise reduction
98 methods, such as filtering or statistical approaches, to improve the image’s clarity. Additionally, color
99 correction techniques are employed to mitigate the color shifts caused by the absorption and scatter-
100 ing of light in water. Another notable approach to underwater image enhancement involves leveraging
101 ML algorithms, particularly DL. Such approaches offer the advantage of adaptability and scalability,
102 as the models can continuously improve with more training data, making them suitable for various
103 underwater imaging applications (Gong et al., 2021).

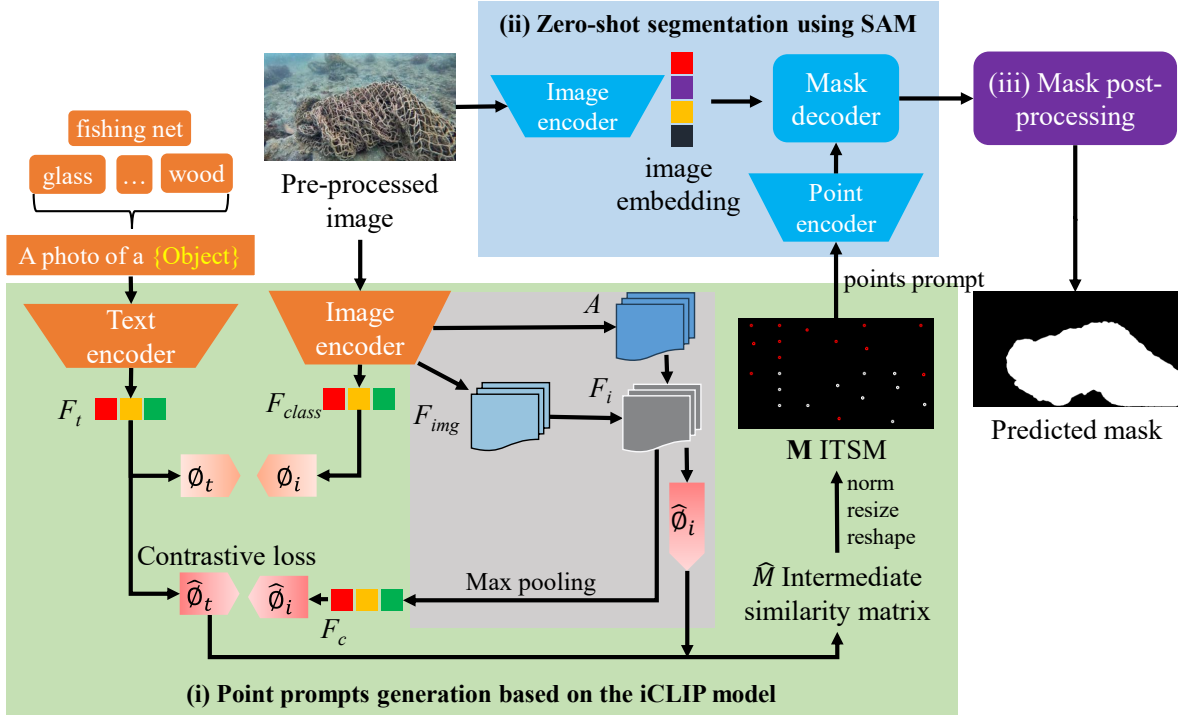
104 The main challenge of previous DL-based UIE is obtaining high-quality ground truth images
105 (Raveendran et al., 2021). Most existing methods generate approximate reference images and train de-
106 terministic enhancement networks that cannot handle the ambiguity of reference mapping. To address
107 the challenge of obtaining high-quality ground truth images for UIE, we implemented a probabilistic
108 network for underwater image enhancement (P-UIE) trained on real-world datasets (Fu et al., 2022).
109 The P-UIE model has two main branches, each implementing a U-Net model with modified SE-ResNet
110 blocks (Gong et al., 2021) for enhanced image feature extraction. The first branch estimates the prior
111 distribution of a single raw underwater image, while the second branch constructs the posterior distri-
112 bution of UIE using the raw underwater image and corresponding reference image as input. The key
113 component of P-UIE is PAdaIN that uses a conditional variational autoencoder (CVAE) (Sohn et al.,
114 2015) and adaptive instance normalization (AdaIN) (Huang and Belongie, 2017) to create a model of
115 the enhancement distribution. During training, random samples from the posterior distribution of the
116 enhanced underwater image are injected into the AdaIN module to transform the enhanced represen-
117 tation. During testing, random samples from the prior distribution are used to make predictions.

118 One of P-UIE’s strengths is its ability to handle the uncertainty of ground truth labels in UIE data.

119 Traditional UIE methods often struggle with this challenge due to noisy and inaccurate ground truth
120 labels. P-UIE's robustness to uncertainty makes it a more reliable UIE method. Another strength of
121 P-UIE is its ability to generate diverse enhanced images from a single input underwater image. This
122 versatility makes P-UIE suitable for a variety of uses, including underwater photography, inspection,
123 and surveillance. As a result, this study implemented a pretrained P-UIE model for enhancing the
124 marine litter dataset before performing the marine litter identification.

125 *3.2. Zero-shot seafloor litter segmentation pipeline*

126 Figure 2 provides a schematic diagram of the proposed zero-shot seafloor litter segmentation
127 pipeline, which consists of three main phases: iCLIP model for point prompt generation, SAM for
128 zero-shot segmentation, and mask post-processing process for removing duplicated masks. iCLIP gen-
129 erates point prompts from an input image and text description of the object of interest, which guide the
130 SAM segmentation model to focus on those regions. However, the obtained masks may contain dupli-
131 cate masks and noise blobs from the background. To address this, we propose a mask post-processing
132 module to eliminate duplication.



Note: Class features are denoted as F_{class} , image features as F_{img} , expanded mean attention map as A , text features as F_t , pooled features as F_c , and masked features as F_i . Additionally, there are dual projections, namely ϕ_i and $\hat{\phi}_i$, along with corresponding text projections, ϕ_t and $\hat{\phi}_t$, used in computing the contrastive losses.

Figure 2: Depiction of the text to points prompt from iCLIP to guide SAM for generating the mask of various types of seafloor litter.

133 3.2.1. Point prompts generation

134 Contrastive Language-Image Pre-training (CLIP) (Radford et al., 2021) is a self-supervised learning
 135 approach that learns to encode images and text into a common representation where semantically
 136 similar images and text are mapped to nearby points. CLIP models have outperformed all other
 137 methods on a variety of downstream vision tasks, including zero-shot classification (Wei et al., 2023),
 138 image retrieval (Saito et al., 2023), and object segmentation (Kirillov et al., 2023). However, the visual
 139 interpretability of CLIP models has been a relatively underexplored area.

140 Li et al. (Li et al., 2022) propose a new interpretable CLIP (iCLIP) model that visualizes the
 141 feature maps of CLIP models. The iCLIP model introduces an Image-Text Similarity Map (ITSM) that

142 computes the similarity between each image’s feature map and the embedding for the corresponding
 143 text description. The ITSM can be used to identify the image regions most relevant to the text
 144 description. Additionally, the authors replace CLIP’s original global pooling layer with a masked max
 145 pooling layer that pools over only the image regions relevant to the text description, as determined by
 146 the ITSM.

147 Given an image sample x and text supervision y , the self-supervised image encoder f_i and linear
 148 projection ϕ_i (a function that learns to project the output of the encoder to a lower dimension) produce
 149 L^p -normalized image token features $\mathbf{X} \in \mathbb{R}^{1+N_i, C}$, as shown in Equation 1.

$$\hat{\mathbf{X}} = f_i(x) \cdot \phi_i, \mathbf{X} = \frac{\hat{\mathbf{X}}}{\|\hat{\mathbf{X}}\|_p} \quad (1)$$

150 where the class token 1 and the image token N_i are represented as vectors in an embedding space
 151 of width C . The feature matrix $\hat{\mathbf{X}}$ contains the features of the image before they are normalized.
 152 Similarly, the normalized text features $\mathbf{Y} \in \mathbb{R}^{N_t, C}$, are computed as shown in Equation 2. These
 153 features are used to train the ITSM model during training and become weights for the ITSM model
 154 during inference.

$$\hat{\mathbf{Y}} = f_t(y) \cdot \phi_t, \mathbf{Y} = \frac{\hat{\mathbf{Y}}}{\|\hat{\mathbf{Y}}\|_p} \quad (2)$$

155 After that, the intermediate similarity matrix $\hat{\mathbf{M}} \in \mathbb{R}^{N_i, N_t}$ is computed by inner production between
 156 image features $\mathbf{X}_{1,:}$ (excluding the class token $\mathbf{X}_{:,1}$;) and the transposed text features \mathbf{Y}^\top , as shown
 157 in Equation 3.

$$\hat{\mathbf{M}} = \mathbf{X}_{1,:} \times \mathbf{Y}^\top \quad (3)$$

158 The ITSM feature map $\mathbf{M} \in \mathbb{R}^{H, W, N_t}$ is then reconstructed reshaping and resizing it to the input
 159 image’s size using bicubic interpolation, with width and height W and H , respectively. Addition-
 160 ally, min-max normalization *Norm* is applied to the H and W dimensions to improve contrast for
 161 visualization. The obtained ITSM can be formulated as follows:

$$\mathbf{M} = \text{Norm}(\text{Resize}(\text{Reshape}(\hat{\mathbf{M}}))) \quad (4)$$

162 For interactive segmentation, iCLIP’s output points with similarity scores higher than 0.8 are used
 163 to guide the SAM model (Li et al., 2022), and the same number of last-ranked points are assigned as
 164 background points. This helps to reduce the need for manual labeling and avoid the poor performance
 165 of SAM with text prompts only.

166 3.2.2. Zero-shot segmentation

167 The Segment Anything Model (SAM) is a new prompt engineering-based semantic segmentation
 168 method introduced by Kirillov et al. (Kirillov et al., 2023). SAM is a promptable model, which means
 169 that it can segment objects in images using a simple prompt. SAM is trained on the SA-1B dataset,
 170 a large dataset of images and text descriptions, and can segment a wide variety of objects, even those
 171 not explicitly defined in the training data.

172 As illustrated in Figure 2(ii), The SAM model architecture consists of three key modules: an image
 173 encoder, a prompt encoder, and a mask decoder. The image encoder processes the input image and
 174 extracts essential visual features that are versatile enough to apply across various object classes in
 175 the context of zero-shot segmentation. It uses vision transformers (ViTs) (Dosovitskiy et al., 2020)
 176 to divide the image into patches and extract features from each patch, capturing both object-specific
 177 details and background information. The prompt encoder can handle two types of prompts: sparse
 178 (points, boxes, and texts) and dense (masks) prompts. Since the location of marine litter in the input
 179 image is unknown, we used the points prompt proposed by the iCLIP model to feed into the prompt
 180 encoder, which encodes the points prompt into a latent representation. Finally, the prompt encoder
 181 output is concatenated with the image encoder output and fed into the mask decoder, which predicts
 182 a segmentation mask for the input image.

183 SAM is trained using a supervised learning approach. The training data consists of images and
 184 text descriptions, where each text description indicates the objects that are present in the image.
 185 SAM is trained to find a minimum cross-entropy loss between the segmentation mask and the actual
 186 segmentation mask.

187 3.2.3. Mask post-processing

188 When points are used as input prompts, the resulting masks often contain many duplicate masks
 189 and noise blobs from the background. To tackle this issue, we implemented a mask post-processing
 190 algorithm (Algorithm 1) in Pseudocode (Nguyen et al., 2023). The algorithm works based on two
 191 parameters: (i) mask area and (ii) overlap ratio. The mask area threshold aims to eliminate excessively
 192 large or small masks that can be considered noise. On the other hand, the overlap ratio is used to
 193 merge masks that are highly similar or substantially overlap into a single mask.

Algorithm 1 Mask post-processing

```

1: selected_masks  $\leftarrow$  []
2: for each mask in sam_output_masks do
3:   mask, mask_area  $\leftarrow$  find_largest_contour(mask)
4:   if  $\min\_area \leq \text{mask\_area} \leq \max\_area$  then
5:     selected_masks  $\leftarrow$  selected_masks  $\cup$  mask
6:   end if
7: end for
8: final_results  $\leftarrow$  []
9: while selected_masks  $\neq$   $\emptyset$  do
10:  pivot_mask  $\leftarrow$  selected_masks.pop() ▷ Assign the last mask from the list to pivot_mask
11:  for each mask in selected_masks do
12:    iou, overlap_ratio  $\leftarrow$  calc_mask_overlap(pivot_mask, mask)
13:    if ( $iou > iou\_threshold$ ) or ( $overlap\_ratio > overlap\_threshold$ ) then
14:      pivot_mask  $\leftarrow$  pivot_mask  $\cup$  mask
15:    end if
16:  end for
17:  final_results  $\leftarrow$  final_results  $\cup$  pivot_mask
18: end while

```

194 Algorithm 1 refines predicted object masks in several steps. Initially, it filters out very small or
 195 large ones based on their area (referred to as *mask_area*). It then iteratively merges overlapping masks
 196 (*selected_mask*). After that, it selects the last mask from the list and stores it in a variable called
 197 *pivot_mask* using the “pop;” operation (which removes the last element from a list). The algorithm
 198 keeps track of the *pivot_mask* and compares it to other masks. If the overlap between the pivot and
 199 another mask exceeds a threshold (either based on IoU or a custom overlap ratio), they are merged
 200 together. This process continues until all masks have been processed. The outcome is a refined list of
 201 masks with reduced noise and merged overlapping detections.

202 4. Experimental results

203 This section describes a series of experiments conducted on the seafloor litter dataset to comprehen-
 204 sively access the performance of the zero-shot segmentation pipeline under different testing conditions.
 205 Section 4.1 details the evaluation metrics used to evaluate the model’s performance on various dimen-
 206 sions, whereas Section 4.2 reports the hardware and programming environment used to implement the
 207 model.

208 4.1. Evaluation metrics

209 Semantic segmentation models are evaluated using a confusion matrix, which has four components:
 210 true positive (TP), true negative (TN), false negative (FN), and false positive (FP). The terms TP ,
 211 TN , FP , and FN refer to the number of pixels that are correctly or incorrectly classified, respectively.
 212 TP is the number of pixels that are correctly predicted to belong to the class of interest, TN indicates
 213 pixels correctly classified as background. FP is the number of pixels that are incorrectly predicted to
 214 belong to a certain class, and FN is the number of pixels that are incorrectly classified as background.
 215 TP , FN , and FP are used to calculate intersection over union (IoU), a popular metric for assessing
 216 model performance. IoU measures how much the predicted segmentation mask overlaps with the
 217 ground truth segmentation mask. Mean IoU (mIoU) is the average IoU over all classes.

$$\begin{aligned} IoU &= \frac{TP}{TP + FP + FN} \\ mIoU &= \frac{IoU}{N} \end{aligned} \quad (5)$$

218 where N is the total number of classes in the dataset, which is 8 in this study.

219 4.2. Implementation descriptions

220 The zero-shot marine litter segmentation framework was developed using PyTorch³, a popular
 221 Python machine learning library, on a Linux system with two Nvidia Tesla V100 GPUs, each with 32
 222 GB of memory. All DL models and hyperparameters, except for the zero-shot segmentation model,

³<https://pytorch.org/>

223 were implemented using open-source code from the original papers. To ensure reliable comparisons
 224 with the zero-shot approach, all supervised segmentation models used a pre-trained ViTs model on
 225 ImageNet as their backbone architecture.

226 4.3. Performance assessment of zero-shot marine litter segmentation framework

227 4.3.1. Pre-processing module analysis

228 Figure 3 shows eight input images from the dataset, which contain various challenges such as low
 229 light, blurriness, and poor illumination. The corresponding outputs from the pre-processing process
 230 show a significant improvement in image quality after passing through the P-UIE model. For example,
 231 marine litter in raw seafloor images with low contrast or poor illumination conditions can be challenging
 232 to see, but the P-UIE model significantly enhances image quality, making marine litter more visible. In
 233 addition, the pre-processing process does not add noise to input images or degrade the quality without
 234 any of the mentioned issues.

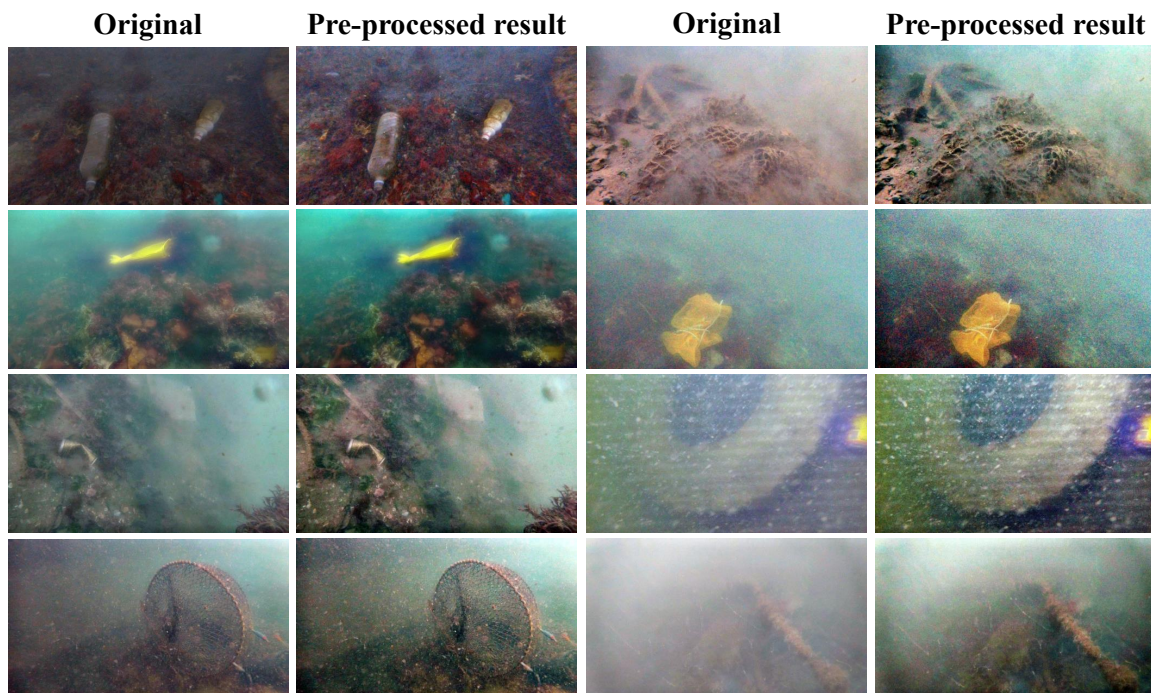


Figure 3: Comparison of the raw and pre-processed seafloor images.

As displayed in Table 1, P-UIE improved the marine litter segmentation performance of the zero-shot approach on three segmentation metrics, including mIoU, precision, and recall. Specifically, the mIoU score increased from 66.2% to 69.9%, the precision score increased from 65.9% to 69.6%, and the recall score increased from 66.7% to 69.8%. This suggests that the P-UIE model was able to effectively improve the quality of the input images, making it easier for the segmentation model to accurately identify and segment the marine litter. In addition, the P-UIE model was able to remove noise and artifacts from the input images, which can make it easier for the segmentation model to distinguish between the marine litter and the background. Finally, the P-UIE model also improved the contrast and color of the input images, which can also make it easier for the segmentation model to identify the marine litter.

Input data	mIoU (%)	Precision (%)	Recall (%)
Raw	66.2	65.9	66.7
Pre-processed	69.9	69.6	69.8

Table 1: The improvement of the pre-processing process on the models' performance.

4.3.2. Zero-shot segmentation performance analysis

Table 2 shows the performance of the proposed zero-shot marine litter segmentation approach for each of the eight marine litter types in the dataset. The table reports the IoU, precision, and recall scores.

	Fishing net	Fish trap	Glass	Metal	Plastic	Wood	Rope	Rubber	Average
IoU	61.5	63.7	75.1	77.2	74.8	70.2	66.4	70.7	70
Precision	60.9	63.3	76.5	75.8	72.2	69.1	68.2	71.4	69.7
Recall	58.9	63.1	77.3	75.7	74.4	71.5	68.7	69.3	69.9

Table 2: Performance of the proposed approach for each marine litter type (IoU, precision, and recall).

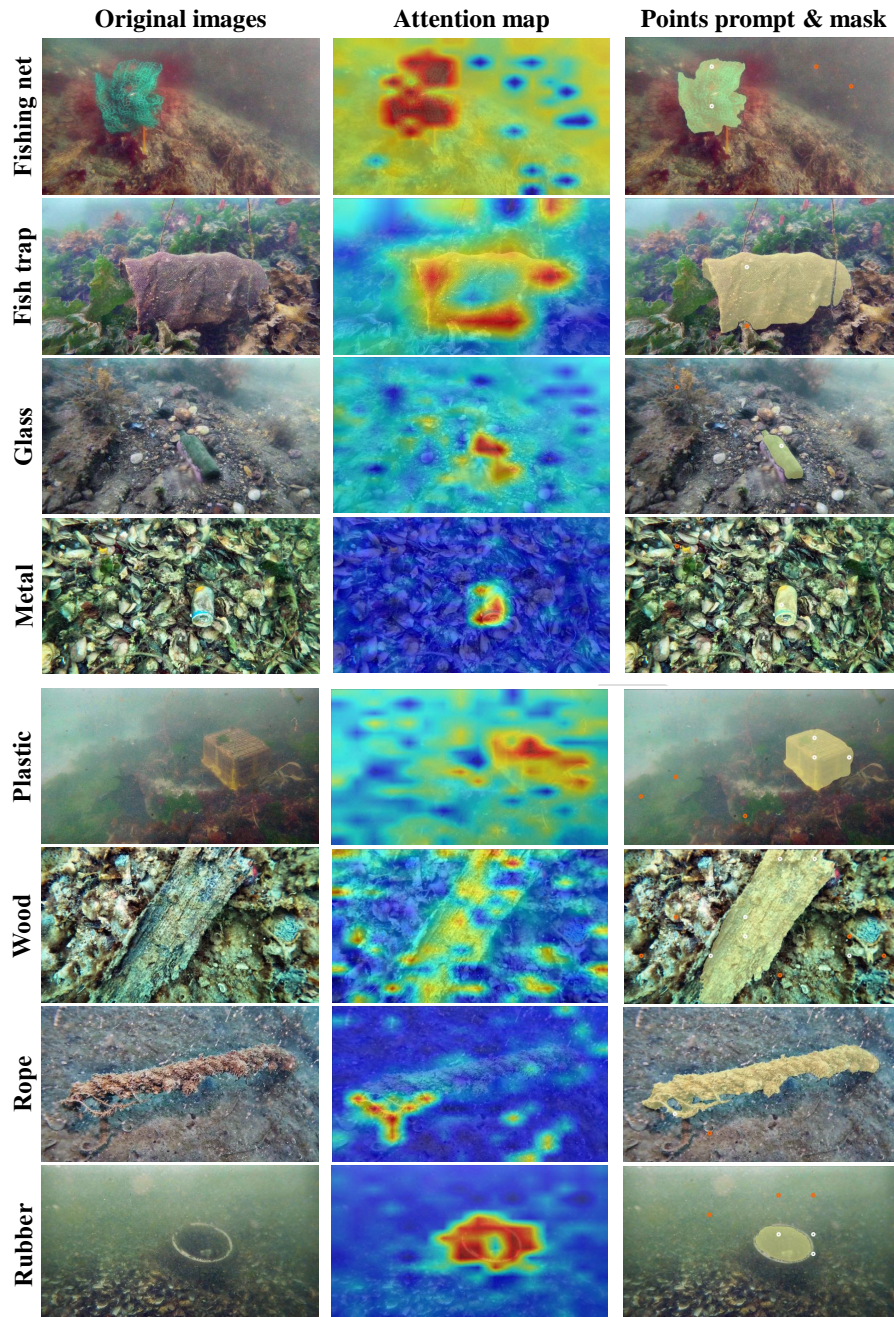
The proposed zero-shot marine litter segmentation approach achieves good performance on all eight marine litter types, with average IoU scores of 70% and average precision and recall scores above 69%. This performance is particularly noteworthy considering that the dataset used in this study was collected on real-life seafloor conditions, which are often challenging for marine litter segmentation algorithms. The highest IoU scores are achieved for metal (77.2%), glass (75.1%), and plastic (74.8%),

254 while the lowest IoU scores are achieved for fishing nets (61.5%) and fish trap (63.7%). This suggests
255 that the proposed approach is a promising approach for zero-shot marine litter segmentation.

256 One possible explanation for the relatively low segmentation performance of fishing nets, fish traps,
257 and ropes is that they can be difficult to distinguish from seaweed and other debris in the environment,
258 especially in low-light or obscured conditions. Additionally, fishing nets and fish traps, which are often
259 made of nylon, can have a similar appearance, further complicating accurate segmentation.

260 Figures 4 shows the model-predicted masks for the eight marine litter types. The first column
261 shows the original image, the second column shows the interpretable CLIP attention masks, which
262 highlight potential litter areas, and the third column shows the overlay of the predicted litter masks
263 on the original image. Overall, the iCLIP attention masks are able to accurately highlight potential
264 litter areas in the image, even in the presence of noise and occlusion. For example, in the case of
265 fishing nets and traps, the attention masks accurately highlight the nets, even when partially obscured
266 by seaweed. Similarly, the attention masks accurately highlight metal, wood, and rubber objects, even
267 when they are similar in color to the surrounding environment.

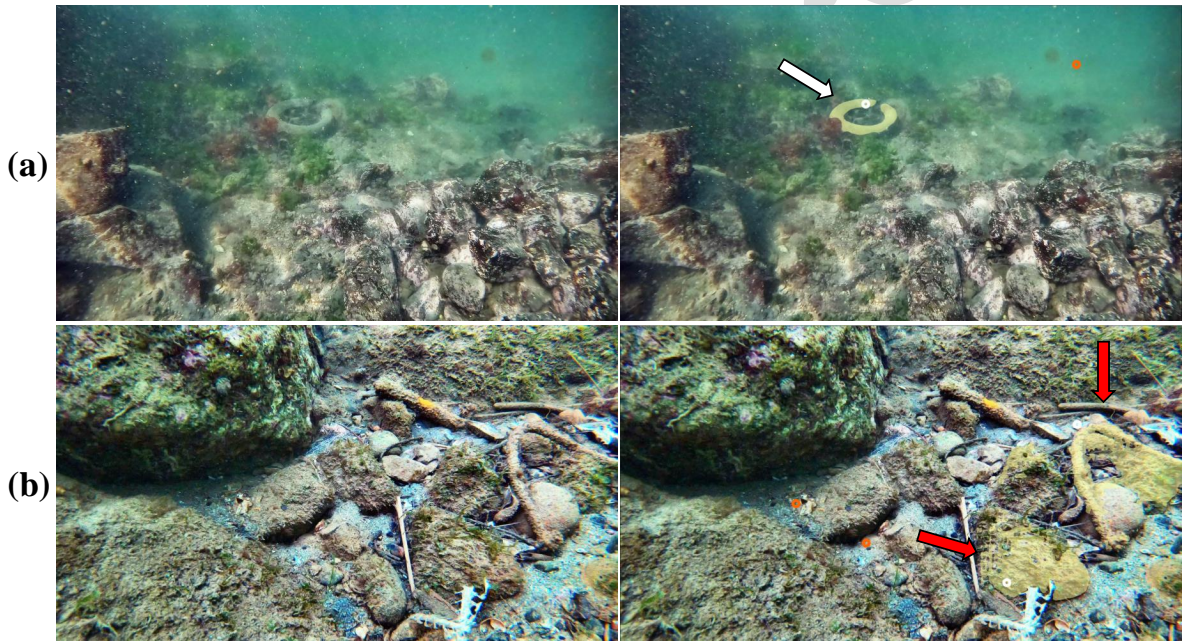
268 Based on the attention masks, the SAM model is guided to accurately segment the litter from
269 the background, closely following the litter boundaries. The SAM model demonstrates potential for
270 accurate object segmentation. While the SAM model generally performs well, it can occasionally
271 exhibit shortcomings, such as incomplete object segmentation or slight over-segmentation.



Note: For each image in the third column, white dots indicating the potential litter areas extracted by the iCLIP model, with red dots indicating the background to guide the SAM model.

Figure 4: Visualization of the proposed zero-shot marine litter segmentation approach on four different types of marine litter.

272 Figure 5 shows the zero-shot segmentation results for two challenging cases where the marine litter
 273 resembles the surroundings. In Figure 5(a), the model correctly segmented the tire, even though it was
 274 small, far from the camera, and had the same color as the surrounding seafloor. However, in Figure
 275 5(b), the model faced a more challenging scenario: the rope resembled the surrounding seafloor rocks,
 276 which is confusing. As a result, the model correctly segmented the rope, but it also falsely recognized
 277 some of the rocks near the rope as rope.



Note: The white arrow indicates correct segmentation, while the red arrow indicates wrong segmentation.

Figure 5: Two examples of marine litter that are challenging to identify due to the complex surrounding environment.

278 4.3.3. Mask post-processing analysis

279 Table 3 displays the mIoU on the testing set obtained from a grid search over various combinations
 280 of mask area (MA) within the range of [5%, 10%, 20%, 30%, 40%] up to 50% of the image area.
 281 Smaller MA values (e.g., 5% or 10%) allow the algorithm to focus on removing tiny masks, which can
 282 be noise or artifacts, whereas larger MA values (e.g., 30% or 40%) aim to eliminate excessively large

283 masks that might cover significant portions of the image. Additionally, we explored overlap thresholds
 284 (OT) ranging from [0.6, 0.7, 0.8, 0.9, 1] for merging duplicated masks. A lower OT (e.g., 0.6 or 0.7)
 285 results in more conservative merging, preserving distinct marine litters. A higher OT (e.g., 0.8 or 0.9)
 286 merges masks more aggressively, potentially combining overlapping marine litters. Our objective was
 287 to identify the parameter combination that maximizes mIoU.

	$MA = 5$	$MA = 10$	$MA = 20$	$MA = 30$	$MA = 40$
$OT = 0.6$	55.5	52.3	54.4	43.9	39.7
$OT = 0.7$	65.1	54.8	51.7	48.1	42.4
$OT = 0.8$	69.9	59.0	58.8	49.6	47.3
$OT = 0.9$	67.3	58.2	58.3	48.8	45.3
$OT = 1$	65.2	55.1	57.5	45.7	44.2

Table 3: Identifying optimal parameters for post-processing process via grid search (MA and OT ranges). The highlighted value shows the best mIoU of the framework on the testing set.

288 The highlighted value represents the best mIoU achieved by the framework on the testing set.
 289 The combination of $MA=5\%$ and $OT=0.8$ yields the highest mIoU of 69.9, indicating effective post-
 290 processing for marine litter segmentation. This setting effectively removes small noise masks while
 291 maintaining reasonable merging thresholds. This optimal parameter combination represents the best
 292 choice for the marine litter dataset.

293 4.3.4. Comparison study for zero-shot segmentation

294 Table 4 shows the performance of the proposed zero-shot segmentation approach on four metrics:
 295 mIoU, precision, recall, and frames per second (FPS), compared to three supervised approaches, in-
 296 cluding Deeplabv3 (Chen et al., 2017), Mask-RCNN (He et al., 2017), and Mask2Former (Cheng et al.,
 297 2022), on the annotated testing dataset. Higher mIoU, precision, and recall indicate more accurate
 298 and complete detection, while higher FPS indicates faster processing speed.

Model	mIoU	Precision	Recall	FPS
DeepLabv3 (Chen et al., 2017)	74.2	75.6	73.7	18
Mask-RCNN (He et al., 2017)	76.1	75.8	77.5	12
Mask2Former (Cheng et al., 2022)	73.8	71.2	72.4	22
Ours (iCLIP+SAM)	69.9	69.6	69.8	16

Table 4: Performance of the zero-shot approach compared to supervised approaches on the annotated testing dataset.

299 Among evaluated models, Mask-RCNN achieves the highest mIoU (76.1%), precision (75.8%), and
300 recall (77.5%). However, it has the slowest inference speed of 12 FPS, making it suitable for offline
301 litter segmentation where time is not a crucial factor. While DeepLabv3, Mask2Former, and the
302 proposed zero-shot approach offer faster inference speeds, their mIoU scores are lower (74.2%, 73.8%,
303 and 69.9%, respectively).

304 The key distinction lies in data requirements. Supervised models like Mask-RCNN, Mask2Former,
305 and DeepLabv3 demand a large-scale labeled dataset for training, which limits their applicability when
306 such data is scarce or unavailable. In contrast, the proposed zero-shot learning approach based on SAM
307 and iCLIP baselines offers a distinct advantage in scenarios where annotated training data is limited or
308 unavailable. In summary, the choice between models depends on the trade-offs between performance
309 and efficiency. Supervised models excel in performance when labeled data is readily available, while
310 the proposed zero-shot approach provides an effective alternative in situations where labeled data is
311 unavailable.

312 5. Discussion

313 Previous studies have shown that the marine environment can have a big impact on the performance
314 of litter detection models. However, they did not offer a solution to this problem. We introduced a
315 pre-processing module based on the P-UIE model to improve the performance of the marine litter
316 segmentation framework. This module is crucial for handling the complexities inherent in marine
317 datasets, leading to a remarkable 3.7% increase in the segmentation model's mIoU, compared to
318 the baseline performance of 66.2% on the raw dataset. While seemingly modest, this improvement
319 translates to a substantial reduction in missed or misclassified marine litter objects within a large-scale
320 dataset. This translates to more precise marine pollution assessments, directly impacting cleanup
321 efforts, ecosystem health monitoring, and research on pollution sources and impacts. While the pre-
322 processing module needs more computing power and time, it can be easily turned on or off depending
323 on the specific needs of the application. Overall, this pre-processing model makes it possible to segment
324 marine litter more effectively in challenging seafloor environments.

325 In this study, we aimed to verify the effectiveness of the zero-shot approach for marine litter seg-
326 mentation. We compared the zero-shot approach with three different DL-based segmentation models
327 on a manually annotated marine litter test set. Our key finding was that the zero-shot approach
328 achieved slightly lower performance (mIoU 69.9%) than other supervised models. The zero-shot ap-
329 proach achieved an inference speed of around 16 FPS, which is affected by the processing speed of the
330 two different models, iCLIP and SAM, as well as the mask post-processing process.

331 Our results are similar to those of previous research on zero-shot approaches. The zero-shot marine
332 litter segmentation pipeline based on iCLIP and SAM has several advantages over traditional super-
333 vised learning approaches, such as Mask-RCNN and DeepLabv3. First, it can be implemented without
334 a large dataset of labeled images, which can be expensive and time-consuming to collect. Second, it is
335 more robust to changes in the appearance of marine litter, such as variations in size, shape, and color.
336 Third, it generalizes well to new environments, such as different water depths and different types of
337 underwater terrain. The proposed zero-shot segmentation algorithm demonstrates promising results
338 in automatically detecting and segmenting marine litter objects in underwater images. The proposed
339 zero-shot marine litter detection framework represents one specific approach within the broader effort
340 to combat marine litter. Our method offers valuable contributions in the field of large-scale monitor-
341 ing of coastal areas, where the model is ready for use for various types of marine litter without the
342 time-consuming process of labeling data and training the model.

343 6. Conclusions and future works

344 Marine litter on the seafloor poses a significant threat, but monitoring it traditionally requires
345 extensive human labor. This research presents a simple yet remarkably efficient framework for au-
346 tomated seafloor litter monitoring. We leverage recent advancements in DL models, particularly in
347 image registration, segmentation, and classification. These advancements have enabled pre-trained
348 models to perform remarkably well in zero-shot learning scenarios. By harnessing the capabilities of
349 these models, we have created a marine litter detection system that stands out for its ability to operate
350 effectively without relying on labeled data or model training.

351 One of the notable innovations proposed in this framework is the utilization of a zero-shot segmen-
352 tation pipeline that includes iCLIP. This technique generates potential points indicating the position of
353 marine litter and the background. These points are then fed into the point prompt encoding of SAM
354 to guide the automated segmentation process. Additionally, we implemented P-UIE, a DL model
355 designed to enhance the visual quality of images captured in underwater environments. Given the
356 challenging underwater conditions, which can sometimes deceive the framework into generating incor-
357 rect object masks, we also introduced a mask post-processing algorithm. This algorithm eliminates
358 erroneous masks based on a carefully fine-tuned IoU threshold and overlap ratio.

359 The framework has been robustly tested and successfully detects eight types of marine litter, even
360 in challenging seafloor environments where distinguishing litter from the background is difficult. It
361 achieved an impressive mIoU of 69.9% and an inference speed of 16 frames per second (FPS). The
362 P-UIE model further improves the mIoU of the pre-processed input from 66.2% to 69.9%. In addition,
363 the extracted attention map serves as a visualization of the model's attention weights. These weights
364 indicate the importance of each pixel in the input image for the model's prediction. This information
365 can be used to understand the model's decision-making process and identify the key features it relies
366 on for making accurate predictions.

367 One notable limitation of the framework is its computational complexity, which hinders real-time
368 litter segmentation. Therefore, optimizing the zero-shot marine litter segmentation framework for
369 both robustness and time efficiency is a crucial area for future research. Additionally, compared to
370 fully supervised segmentation models like Mask-RCNN and DeeplabV3, the proposed model exhibited
371 lower accuracy for recognizing underwater marine litter with fine-grained details and subtle variations.
372 One possible direction is to combine the zero-shot framework with limited amounts of marine litter
373 detection-specific labeled data (few-shot learning) or incorporating active learning strategies to improve
374 accuracy and reduce reliance on large pre-trained models. In addition to technological advancements,
375 promoting complementary strategies is essential for tackling marine litter effectively. These strategies
376 can include improved waste management infrastructure, educational initiatives promoting responsible
377 waste disposal, and policy changes encouraging sustainable practices.

378 **CRedit authorship contribution statement**

379 **Tri-Hai Nguyen:** Writing – original draft, Investigation, Formal analysis, Visualization. **L. Minh**

380 **Dang:** Data curation, Validation, Writing – review & editing.

381 **Declaration of Competing Interest**

382 The authors declare that they have no known competing financial interests or personal relationships
383 that could have appeared to influence the work reported in this paper.

384 **Data availability**

385 The data is publicly available on <https://www.aihub.or.kr/>

386 **References**

387 , . Deep-sea debris database. <https://www.godac.jamstec.go.jp/dsdebris/e/index.html>. Ac-
388 cessed: September 21, 2023.

389 , . Hero5 black. <https://gopro.com/en/us/update/hero5-black>. Accessed: September 27, 2023.

390 Chen, L.C., Papandreou, G., Schroff, F., Adam, H., 2017. Rethinking atrous convolution for semantic
391 image segmentation. arXiv preprint arXiv:1706.05587 .

392 Cheng, B., Misra, I., Schwing, A.G., Kirillov, A., Girdhar, R., 2022. Masked-attention mask trans-
393 former for universal image segmentation, in: Proceedings of the IEEE/CVF conference on computer
394 vision and pattern recognition, pp. 1290–1299.

395 Chin, C.S., Neo, A.B.H., See, S., 2022. Visual marine debris detection using yolov5s for autonomous
396 underwater vehicle, in: 2022 IEEE/ACIS 22nd International Conference on Computer and Informa-
397 tion Science (ICIS), IEEE. pp. 20–24.

398 Corrigan, B.C., Tay, Z.Y., Konovessis, D., 2023. Real-time instance segmentation for detection of
399 underwater litter as a plastic source. Journal of Marine Science and Engineering 11, 1532.

- 400 Deng, H., Ergu, D., Liu, F., Ma, B., Cai, Y., 2021. An embeddable algorithm for automatic garbage
401 detection based on complex marine environment. *Sensors* 21, 6391.
- 402 Dosovitskiy, A., Beyer, L., Kolesnikov, A., Weissenborn, D., Zhai, X., Unterthiner, T., Dehghani, M.,
403 Minderer, M., Heigold, G., Gelly, S., et al., 2020. An image is worth 16x16 words: Transformers for
404 image recognition at scale. arXiv preprint arXiv:2010.11929 .
- 405 Fu, Z., Wang, W., Huang, Y., Ding, X., Ma, K.K., 2022. Uncertainty inspired underwater image
406 enhancement, in: *European Conference on Computer Vision*, Springer. pp. 465–482.
- 407 Galgani, L., Beiras, R., Galgani, F., Panti, C., Borja, A., 2019. Impacts of marine litter.
- 408 Gong, L., Du, X., Zhu, K., Lin, C., Lin, K., Wang, T., Lou, Q., Yuan, Z., Huang, G., Liu, C., 2021.
409 Pixel level segmentation of early-stage in-bag rice root for its architecture analysis. *Computers and*
410 *Electronics in Agriculture* 186, 106197.
- 411 He, K., Gkioxari, G., Dollár, P., Girshick, R., 2017. Mask r-cnn, in: *Proceedings of the IEEE interna-*
412 *tional conference on computer vision*, pp. 2961–2969.
- 413 Huang, B., Chen, G., Zhang, H., Hou, G., Radenkovic, M., 2023. Instant deep sea debris detection for
414 maneuverable underwater machines to build sustainable ocean using deep neural network. *Science*
415 *of the Total Environment* 878, 162826.
- 416 Huang, X., Belongie, S., 2017. Arbitrary style transfer in real-time with adaptive instance normaliza-
417 tion, in: *Proceedings of the IEEE international conference on computer vision*, pp. 1501–1510.
- 418 Iñiguez, M.E., Conesa, J.A., Fullana, A., 2016. Marine debris occurrence and treatment: A review.
419 *Renewable and Sustainable Energy Reviews* 64, 394–402.
- 420 Jang, Y.C., Lee, G., Kwon, Y., Lim, J.h., Jeong, J.h., 2020. Recycling and management practices of
421 plastic packaging waste towards a circular economy in south korea. *Resources, Conservation and*
422 *Recycling* 158, 104798.
- 423 Jia, T., Kapelan, Z., de Vries, R., Vriend, P., Peereboom, E.C., Okkerman, I., Taormina, R., 2023.
424 Deep learning for detecting macroplastic litter in water bodies: A review. *Water Research* , 119632.

- 425 Jian, M., Liu, X., Luo, H., Lu, X., Yu, H., Dong, J., 2021. Underwater image processing and analysis:
426 A review. *Signal Processing: Image Communication* 91, 116088.
- 427 Kirillov, A., Mintun, E., Ravi, N., Mao, H., Rolland, C., Gustafson, L., Xiao, T., Whitehead, S., Berg,
428 A.C., Lo, W.Y., et al., 2023. Segment anything. *arXiv preprint arXiv:2304.02643* .
- 429 Kraft, M., Piechocki, M., Ptak, B., Walas, K., 2021. Autonomous, onboard vision-based trash and
430 litter detection in low altitude aerial images collected by an unmanned aerial vehicle. *Remote Sensing*
431 13, 965.
- 432 Li, Y., Wang, H., Duan, Y., Xu, H., Li, X., 2022. Exploring visual interpretability for contrastive
433 language-image pre-training. *arXiv preprint arXiv:2209.07046* .
- 434 Ma, D., Wei, J., Li, Y., Zhao, F., Chen, X., Hu, Y., Yu, S., He, T., Jin, R., Li, Z., et al., 2023. Mldet:
435 Towards efficient and accurate deep learning method for marine litter detection. *Ocean & Coastal*
436 *Management* 243, 106765.
- 437 Madricardo, F., Ghezzi, M., Nesto, N., Mc Kiver, W.J., Faussone, G.C., Fiorin, R., Riccato, F.,
438 Mackelworth, P.C., Basta, J., De Pascalis, F., et al., 2020. How to deal with seafloor marine litter:
439 an overview of the state-of-the-art and future perspectives. *Frontiers in Marine Science* 7, 505134.
- 440 Mæland, C.E., Staube-Delgado, R., 2020. Can the global problem of marine litter be considered a
441 crisis? *Risk, Hazards & Crisis in Public Policy* 11, 87–104.
- 442 Marin, I., Mladenović, S., Gotovac, S., Zaharija, G., 2021. Deep-feature-based approach to marine
443 debris classification. *Applied Sciences* 11, 5644.
- 444 Minh, D., Wang, H.X., Li, Y.F., Nguyen, T.N., 2022. Explainable artificial intelligence: a comprehen-
445 sive review. *Artificial Intelligence Review* , 1–66.
- 446 Nguyen, L.Q., Shin, J., Ryu, S., Dang, L.M., Park, H.Y., Lee, O.N., Moon, H., 2023. Innovative
447 cucumber phenotyping: A smartphone-based and data-labeling-free model. *Electronics* 12, 4775.

- 448 Politikos, D.V., Fakiris, E., Davvetas, A., Klampanos, I.A., Papatheodorou, G., 2021. Automatic
449 detection of seafloor marine litter using towed camera images and deep learning. *Marine Pollution*
450 *Bulletin* 164, 111974.
- 451 Radeta, M., Zuniga, A., Motlagh, N.H., Liyanage, M., Freitas, R., Youssef, M., Tarkoma, S., Flores,
452 H., Nurmi, P., 2022. Deep learning and the oceans. *Computer* 55, 39–50.
- 453 Radford, A., Kim, J.W., Hallacy, C., Ramesh, A., Goh, G., Agarwal, S., Sastry, G., Askell, A., Mishkin,
454 P., Clark, J., et al., 2021. Learning transferable visual models from natural language supervision,
455 in: *International conference on machine learning*, PMLR. pp. 8748–8763.
- 456 Raveendran, S., Patil, M.D., Birajdar, G.K., 2021. Underwater image enhancement: a comprehensive
457 review, recent trends, challenges and applications. *Artificial Intelligence Review* 54, 5413–5467.
- 458 Saito, K., Sohn, K., Zhang, X., Li, C.L., Lee, C.Y., Saenko, K., Pfister, T., 2023. Pic2word: Map-
459 ping pictures to words for zero-shot composed image retrieval, in: *Proceedings of the IEEE/CVF*
460 *Conference on Computer Vision and Pattern Recognition*, pp. 19305–19314.
- 461 Sandra, M., Devriese, L.I., Booth, A.M., De Witte, B., Everaert, G., Gago, J., Galgani, F., Langedock,
462 K., Lusher, A., Maes, T., et al., 2023. A systematic review of state-of-the-art technologies for
463 monitoring plastic seafloor litter. *Journal of Ocean Engineering and Science* .
- 464 Schneider, F., Parsons, S., Clift, S., Stolte, A., McManus, M.C., 2018. Collected marine litter—a
465 growing waste challenge. *Marine pollution bulletin* 128, 162–174.
- 466 Sohn, K., Lee, H., Yan, X., 2015. Learning structured output representation using deep conditional
467 generative models. *Advances in neural information processing systems* 28.
- 468 Sun, X., Gu, J., Sun, H., 2021. Research progress of zero-shot learning. *Applied Intelligence* 51,
469 3600–3614.
- 470 Teng, C., Kylili, K., Hadjistassou, C., 2022. Deploying deep learning to estimate the abundance of
471 marine debris from video footage. *Marine Pollution Bulletin* 183, 114049.

- 472 Wei, Y., Cao, Y., Zhang, Z., Peng, H., Yao, Z., Xie, Z., Hu, H., Guo, B., 2023. iclip: Bridging image
473 classification and contrastive language-image pre-training for visual recognition, in: Proceedings of
474 the IEEE/CVF Conference on Computer Vision and Pattern Recognition, pp. 2776–2786.
- 475 Zhou, W., Zheng, F., Yin, G., Pang, Y., Yi, J., 2022. Yolotrashcan: A deep learning marine debris
476 detection network. IEEE Transactions on Instrumentation and Measurement 72, 1–12.

Highlights

- We introduce a zero-shot marine litter segmentation framework
- An underwater image enhancement algorithm was applied to improve the dataset quality
- The framework achieves a test mIOU of 69.9% for eight common marine litter
- We perform detailed analysis of the model's robustness against complex background noise
- We demonstrate the potential of zero-shot approach for automated marine litter monitoring

Declaration of interests

The authors declare that they have no known competing financial interests or personal relationships that could have appeared to influence the work reported in this paper.

The authors declare the following financial interests/personal relationships which may be considered as potential competing interests:

Journal Pre-proof